

Spin measurements in cascade decays at the LHC

Lian-Tao Wang and Itay Yavin

*Jefferson Physical Laboratory, Harvard University,
Cambridge, MA 02138, U.S.A.*

E-mail: lianwang@Princeton.edu, iyavin@princeton.edu

ABSTRACT: We systematically study the possibility of determining the spin of new particles after their discovery at the LHC. We concentrate on angular correlations in cascade decays. Motivated by constraints of electroweak precision tests and the potential of providing a Cold Dark Matter candidate, we focus on scenarios of new physics in which some discrete symmetry guarantees the existence of stable neutral particles which escape the detector. More specifically, we compare supersymmetry with another generic scenario in which new physics particles have the same spin as their Standard Model partners. A survey of possibilities of observing spin correlations in a broad range of decay channels is carried out, with interesting ones identified. Rather than confining ourselves to one “collider friendly” benchmark point (such as SPS1a), we describe the parameter region in which any particular decay channel is effective. We conduct a more detailed study of chargino’s spin determination in the decay channel $\tilde{q} \rightarrow q + \tilde{C}^\pm \rightarrow q + W^\pm + LSP$. A scan over the chargino and neutralino masses is performed. We find that as long as the spectrum is not too degenerate the prospects for spin determination in this channel are rather good.

KEYWORDS: Hadron-Hadron Scattering.

Contents

1. Introduction	1
2. Simple spin correlations	4
2.1 Scalar decay	5
2.2 Fermion decay	5
2.3 Gauge-boson decay	6
2.4 Higher spin	7
3. Angular correlations in cascade decays	7
3.1 Weak decay with $q\ell^\pm$ final state	8
3.2 Weak decay with $q\bar{q}$ final states	11
3.3 Weak decay with qW^\pm final state	11
3.4 Weak decay with qZ final state	12
3.5 Weak decay with qh final state	13
3.6 Decay of gluon partner	13
3.7 Strong decay of quark partner	14
3.8 Decay from leptonic initial states	15
3.9 Off-shell decays	15
4. Determining spin without leptonic partners	16
4.1 Experimental observable - lepton-jet correlation	18
4.2 Experimental observable - jet- W correlation	20
4.3 Scanning M_1 and M_2	24
5. Conclusions and future directions	25
A. Matrix elements calculations	27
B. HERWIG implementation	29

1. Introduction

Naturalness of the weak scale implies the existence of new physics beyond the Standard Model at the scale \sim TeV. Typical new physics scenarios predict the existence of a set of new particles at that scale. The Large Hadron Collider (LHC) gives us a great opportunity for discovering those particles.

In order to understand the nature of the new physics, it is necessary to measure its properties in detail. One of the obvious tasks is to reconstruct the masses [1–8] and

gauge quantum numbers of the new particles from experimental data. A recent study [9] demonstrated the challenges of such a goal and suggested possible directions in achieving it.

On the other hand, there is another, at least equally important, LHC inverse problem: how do we determine the spin of any newly discovered particle? The proposed new particles in several main candidates of new physics scenarios typically have similar gauge interactions. They could often be organized as partners of the known Standard Model particles with the same gauge quantum number, such as quark partners, lepton partners and gauge boson partners. A typical example is the set of superpartners in supersymmetry, including squarks, sleptons, gauginos, and so on. Another interesting scenario is the theory space models inspired by [10]. The duplication of the Standard Model states in this scenario comes from introducing more copies of the Standard Model gauge group. Typical examples are little Higgs models.¹ Measuring the partners' spin becomes a crucial, sometimes single, way to distinguish those scenarios.

Motivated by electroweak precision constraints and the existence of Cold Dark Matter, many new physics scenarios incorporate some discrete symmetry which guarantees the existence of a lightest stable neutral particle, LSNP. Well-known examples of such discrete symmetries include R-parity in supersymmetry, KK-parity in universal extra-dimension models [11], or similarly, T-parity in Little Higgs Models [12–15]. The existence of such a neutral particle at the end of the decay chain results in large missing energy events in which new physics particles are produced. This fact helps to separate them from the Standard Model background. On the other hand, it also makes the spin measurement more complicated because it is almost impossible to reconstruct the momentum, and therefore the rest frame, of the decaying particles.

The question of spin determination has been revisited recently. The total cross section might serve as an initial hint to the spin of the new particles discovered [16]. This is not entirely satisfactory because certain model dependence is inevitable when using the rate information. For example, a fermion can be faked by two closely degenerate scalars. Moreover, such a determination is only possible if we could measure the masses of the particle using kinematical information. As demonstrated in [15, 17], typical “transverse” kinematical observables are not sensitive to the absolute mass of particles. One can only deduce the mass difference between the decaying particle and the neutral particle escaping the detector. With some assumptions regarding the underlying model there are more subtle kinematical observables which, in combination with the rate information, could determine the spin [17]. To what extent this could be generalized to a broader classes of new physics particles is currently under investigation.

Therefore, it is important to investigate other possible ways of directly measuring the spin of new particles. The typical way of measuring the spin of a decaying particle starts with reconstructing its rest frame from the decay products. Then, the angular distribution in the rest frame contains the full spin information, independent of the boost. As discussed

¹Another well-known example is the the extra-dimensional setup with the corresponding KK particles. As we learned in the past few years, this is related to the theory space models via deconstruction

above, we do not have enough kinematical information to boost to the rest frame of the decaying particle if the spectrum contains a LSNP. Therefore, it is natural to consider distributions as a function of relativistic invariants constructed out of the decay products of a single decaying particle. We will focus on this possibility in this paper.

Various new physics models always have some detailed differences in their spectra. But, such differences are very model dependent. Although in principle they could carry interesting information, we will focus on spin determination based on Standard Model partners only. What we have in mind are two classes of models with almost identical gauge quantum numbers and maximal flexibility in their mass spectra. In other words, they would look very similar except for their spin content.

One obvious scenario is low energy supersymmetry, parameterized by the MSSM with a conserved R-parity.

As a contrasting scenario we consider a framework in which all new particles have the same spin as their Standard Model counter parts. The existence of a LSNP, is guaranteed by the assumption that all the new physics particles are odd under a certain Z_2 parity. Special cases of this scenario could be the first KK level of UED or T-parity little Higgs. However, what we have in mind is a more generic setup and we will not constrain ourselves to any special mass or coupling relations imposed by these two scenarios. To emphasize its generic nature, we will call it the Same Spin scenario in this paper. We will use symbols with primes to label the new particles in the Same Spin scenario. For example, we will use q' to label the quark partner, and so on. We will assume the LSNP in this case is a vector and label it as A' .

Typical new physics scenarios have many complicated decay channels. Many kinematical distributions can be constructed from them. One of the main goals of this paper is to present a systematic survey of the observability of spin correlations in a wide variety of decay chains which are generically present in new physics scenarios. We identify interesting decay channels to focus on for spin measurements. It is important to notice, as will be clear from our discussion, that the usefulness of any particular channel is restricted to a specific range of parameters. We describe the kinematical requirements for each of the channels we analyze. There is no obvious golden channel. For different points in the parameter space, we will generically have different decay channels available. Therefore, we will have to devise different strategies depending on mass spectra of underlying models.

One of the important tools we develop in this paper is a set of simple rules, which summarizes many well-known results concerning spin correlations. Such simple rules allows one to gain insight into the angular correlations in decay, without the necessity of going through a lengthy calculation. They can be useful in other, potentially more complicated, scenarios than the ones considered hereafter.

Barr [18] investigated a typical supersymmetry cascade involving a squark decay. He found that angular correlations exist between the decay products. Barr's method relies on the fact that squarks and anti-squarks are produced unevenly in a proton-proton collider. There are several follow-up studies along the same lines [19–21]. References [20] and [19] went further and contrasted supersymmetry with the universal extra-dimensions scenario [11, 22]. Reference [20] found that with a mass spectrum given by the SPS point

1a, the SUSY model is distinguishable from the UED case. In their study, they assumed the lepton can be perfectly correlated with the correct jet. That might be possible if complete kinematic information is available, but in practice seems quite difficult. In general jet combinatorics must be taken into account.

One limitation of these investigations is the need for a light leptonic partner. It must be lighter than the second lightest neutral gauge boson partner, such as the second lightest neutralino (which must be a wino or bino), in supersymmetry. While true in some special benchmark models [23], there is no reason to assume this is a generic feature of supersymmetry breaking. In fact, it is more generic to assume otherwise, especially if one is driven by the problem of naturalness.

We present a detailed study of spin correlations in the decay chain $\tilde{q} \rightarrow q + \tilde{C}_1^\pm \rightarrow q + W^\pm + \tilde{N}_1$ in supersymmetry and its counter part $q' \rightarrow q + W'^\pm \rightarrow q + W^\pm + A'$ in the Same Spin scenario. Such a decay chain does not require the leptonic partner to be lighter than the gauge boson partner and is certainly more generic in parameter space. We will assume that the mass splitting between the two lightest states is greater than $m_{W,Z}$. Therefore, the on-shell decay to W/Z always dominates.² Our result shows that it is possible to observe spin correlation in this decay chain. As a demonstration of the result of our general discussion, we map out the parameter region in which this decay channel is useful.

As part of the analysis we used HERWIG 6.507 [24] which implements a spin correlation algorithm. This algorithm was first used for QCD parton showers [25–28] and later extended by Richardson to supersymmetric and top processes [29]. We supplemented the code to include the decays of massive gauge bosons (such as KK partners of the gluon) and the details are spelled out in appendix B. To the best of the authors' knowledge, HERWIG is the only simulator that implements such an algorithm and is therefore suitable for spin determination studies.

The paper is organized as follows: In section 2 we try to build some intuition by looking at the effects of spin on the angular distributions of simple decays. In section 3, we present a survey of spin correlations in various decay channels. Our detailed study of the decay chain with qW^\pm final states is presented in section 4. There, we take up the task of constructing an observable signal to distinguish SUSY from the Same Spin scenario in the absence of any leptonic partners. Finally, in section 5, we comment on possible future directions and present our conclusions.

2. Simple spin correlations

In this section we review some basic angular distributions from simple decays. These distributions will serve as building blocks in our understanding of the spin correlations in more complicated decay chains which we will consider later.

²If the mass splitting is less than $m_{W,Z}$, sometimes, the off-shell diagram via a squark and slepton can be important. Although it is a special case of the mass spectrum, it is certainly worthwhile exploring it further.

2.1 Scalar decay

A scalar does not pick any special direction in space and so its decay is isotropic. It does not mean that the existence of scalars spoils any hope for distinguishing them away from phase-space. The production of bosons (via a Z^0 for example) has a different angular distribution about the beam axis than that of fermions. This discrepancy can be employed in determining the spin of lepton partners (see for example, [30]). However, in our study we will concentrate on a single branch in which case it is not possible to distinguish a scalar from phase-space.

2.2 Fermion decay

First, we consider the decay of a fermion ψ_1 into another fermion ψ_2 and a scalar ϕ , via an interaction of the form

$$y_L \phi \bar{\psi}_2 P_L \psi_1 + y_R \phi \bar{\psi}_2 P_R \psi_1 \tag{2.1}$$

Depending on the model, this coupling could be either chiral, $y_L \neq y_R$, or non-chiral, $y_L = y_R$. We will see examples of both cases in our study.

If the coupling in eq. 2.1 is chiral, ψ_2 is produced in a chirality eigenstate. If ψ_2 is boosted then it is in a helicity eigenstate, i.e., polarized. However, ψ_1 is, in general, not polarized and therefore the decay is isotropic, even if the coupling (2.1) is chiral and ψ_2 is boosted. It is easy to see how this comes about. If it is a Left handed coupling, $y_R = 0$, then ψ_2 is mostly a right-handed particle, $|\downarrow\rangle$. From the transformation of a spinor under a rotation by an angle θ we have that,

$$\begin{aligned} |\uparrow\rangle &\rightarrow \cos\left(\frac{\theta}{2}\right) |\uparrow\rangle + \sin\left(\frac{\theta}{2}\right) |\downarrow\rangle \\ |\downarrow\rangle &\rightarrow -\sin\left(\frac{\theta}{2}\right) |\uparrow\rangle + \cos\left(\frac{\theta}{2}\right) |\downarrow\rangle \end{aligned}$$

The angle θ is defined with respect to ψ_1 polarization axis. Notice that if ψ_1 is left-handed polarized, $|\uparrow\rangle$, its decay probability is $\propto \sin^2\left(\frac{\theta}{2}\right)$. On the other hand, if it is right-handed polarized, $|\downarrow\rangle$, its decay probability $\propto \cos^2\left(\frac{\theta}{2}\right)$. These decay distributions are shown in figure (1) as a function of $\cos(\theta)$. Unfortunately, ψ_1 itself is normally not polarized and averaging over the two process the decay is indeed isotropic.

However, if ψ_1 came from the decay of another particle and that vertex was chiral then the situation is different. In that case ψ_1 is polarized and its subsequent decay is governed by a non-trivial angular distribution as shown in figure (1). Whether the decay involves a helicity flip or not determines the sign of the slope.

Next, we consider the decay of a fermion into another fermion and a gauge-boson via an interaction of the form

$$g_L \bar{\psi}_2 \gamma^\mu P_L \psi_1 A_\mu + g_R \bar{\psi}_2 \gamma^\mu P_R \psi_1 A_\mu \tag{2.2}$$

As before, we consider the case where ψ_2 is boosted. If the interaction is chiral ψ_2 is in a definite helicity state. The fermionic current that couples to A^μ is of the form $\bar{\psi}_\alpha \sigma_\mu^{\dot{\alpha}\beta} \psi_\beta$. If the emitted gauge-boson is longitudinally polarized the distributions are the same as the

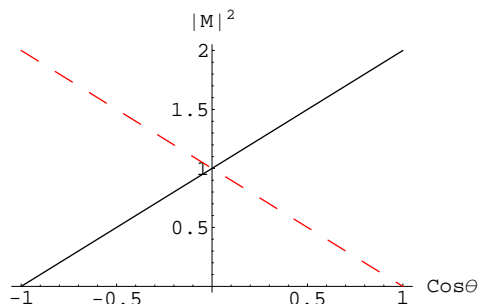


Figure 1: The decay probability for a fermion into a scalar and another fermion of the same helicity (solid-black) or opposite helicity (dashed-red) as a function of $\cos\theta$. θ is defined with respect to the axis of polarization of the decaying fermion.

decay into a fermion and a scalar. If it transversely polarized it is precisely opposite (i.e. same helicity corresponds to $\sin^2\theta/2$ and opposite helicity to $\cos^2\theta/2$).

The most important feature of the fermion’s decay is the linear dependence of the decay probability on $\cos\theta$. It is also clear that chiral vertices must be involved in order to observe spin correlations (unless the fermion is a Majorana particle, a possibility we discuss below).

2.3 Gauge-boson decay

When a gauge-boson decay (2-body), relativity forces the products to be two bosons or two fermions. As is well known, when the products are two fermions the angular distribution is given by,

$$P_{\text{trans}}(\cos\theta) = \frac{1}{4}(1 + \cos^2\theta) \quad P_{\text{long}}(\cos\theta) = \frac{1}{2}(1 - \cos^2\theta) \quad (2.3)$$

If a gauge boson decays into two scalars via the interaction

$$g\phi_2^* \overleftrightarrow{\partial}_\mu \phi_1 A^\mu, \quad (2.4)$$

the angular distribution has the opposite structure,

$$P_{\text{trans}}(\cos\theta) = \frac{1}{2}(1 - \cos^2\theta) \quad P_{\text{long}}(\cos\theta) = \cos^2\theta \quad (2.5)$$

where the subscript on P denotes the initial gauge-boson’s polarization. As usual θ is defined about the polarization axis. The decay of a gauge-boson into two other gauge-bosons has the same angular distribution as eq. (2.5). These are shown in figure (2). As usual there are finite mass effects that come into play when the products are not highly boosted. Those tend to wash out any angular dependence of the amplitude. Generically these contributions scale as m^2/E^2 . Therefore, as noted before there has to be an appreciable difference between the mass of the decaying particle and its products so that $m^2/E^2 \lesssim 1/2$.

The contrast with the previous case is clear as the dependence of the amplitude on $\cos\theta$ is quadratic. It is also important to note that the vertex need not be chiral.

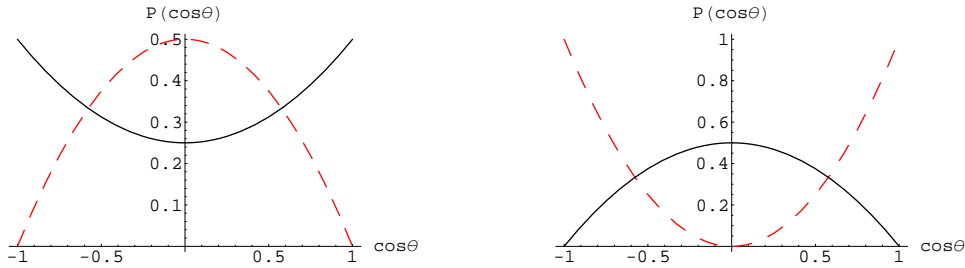


Figure 2: The decay probability for a gauge-boson into two fermions (left) and two bosons (right) for transverse (solid-black) and longitudinal polarization (dashed-red) as a function of $\cos\theta$.

2.4 Higher spin

By noting that a rotation by θ of a state of spin j is given by $e^{i\theta j\sigma_y}$ it is easy to see that the amplitude for the decay of a particle with spin j is some polynomial of degree $2j$,

$$P_\lambda(\cos\theta) = a_{2j}(\cos\theta)^{2j} + a_{2j-1}(\cos\theta)^{2j-1} + \dots + a_0 \quad (2.6)$$

The coefficients a_i are such that when we sum over all polarizations λ we get,

$$\sum_\lambda P_\lambda(\cos\theta) = 1 \quad (2.7)$$

since an unpolarized particle has no preferred direction. In this paper we concentrate on spin $0, 1/2$, and 1 and will not consider higher spin. Nonetheless, this is an important issue to address. For example, if the partners of the graviton are indeed detected it would be good to know whether it is a supersymmetric spin- $3/2$ object or a Same-Spin spin- 2 resonance.

3. Angular correlations in cascade decays

In this section, we present a systematic study of spin correlations in a wide variety of cascade decay channels. Aside from the matrix element, the kinematics also play a crucial role in the observability of spin effects. We lay out the conditions for observing spin correlations in each of the decay channels we discuss. Whether any of the channels is open or not depends on the particular mass spectrum. However, it is not unreasonable to expect several such channels to be open in a generic model. This is important because the signal from any one channel might not be sufficiently strong. In this case we would have to combine the signal from a few channels to obtain a high confidence spin determination.

We focus on a class of specific kinematical observables. It is constructed from the momenta of two of the observed final state particles. More complicated decay patterns and observables consisting of more than two observable particles could also be interesting.

A generic feature of this type of observables is that spin information of the *intermediate* particle, which has observable decay products on both sides, in the decay chain always manifest itself as some polynomial structure in the distribution. Indeed, a particle of spin

j , if polarized, will result in a polynomial of degree $2j$. On the other hand, such a method is not useful for determining the spin of any particle at the top or bottom of the decay chain. For the same reason, very short decay chains such as $\tilde{q} \rightarrow q + \text{LSP}$ won't contain much information.

As discussed in section 2, a key requirement for the existence of any spin correlations is for the intermediate state particle to be polarized.³ A boost invariant way to know whether a particle is polarized or not is to study this question in its rest frame using a direction defined by its mother particle and the other decay products. We will see examples of such analysis in the decay channels we consider below. From the discussion in the previous section, it is clear that there are only a few ways for a particle to be polarized in its rest frame,

1. For Majorana fermions a spin flip results in a different process with different end products. We must be able to tell those apart (measuring a leptons vs. anti-lepton). We will see this in detail in the discussion to follow.
2. Dirac fermions must be produced from a (partially) chiral coupling and decay through a (partially) chiral interaction.
3. In general the spectrum of new particles needs not be left-right symmetric. In this case, the interaction of these particles is effectively chiral even if the gauge-coupling is vector like. A typical example is the asymmetric QCD production of left and right squarks when their masses are very different.⁴
4. For a gauge boson, it must come from the decay of a boosted particle (in the gauge-boson rest frame).

We will see detailed realizations of all of these requirements in various decay channels we study in this section.

We will organize our discussion in terms of different final states.

3.1 Weak decay with $q\ell^\pm$ final state

We will go through the logic of establishing spin correlation this channel in more detail because many other channels can be understood following very similar arguments.

We first consider the supersymmetric case. Here, the decay to $q\ell^\pm$ final states will proceed through either Dirac or Majorana fermion intermediate states. We consider the case of a Dirac fermion first (i.e., chargino intermediate state) and compare it with the corresponding process in the Same Spin scenario where the intermediate state is a massive gauge boson W' . We will comment on the case of Majorana fermion briefly. For more details, see [18].

In the case of a Dirac fermion there are two possible ways for the particle to be polarized. If it is off-shell then one of the helicities dominates over the other simply

³Strictly speaking, this requirement only applies for on-shell particles. For off-shell particles, the spin correlation could have new interesting properties. We will examine the off-shell decay in section 3.9

⁴We would like to thank M. Peskin for bringing this fact to our attention.

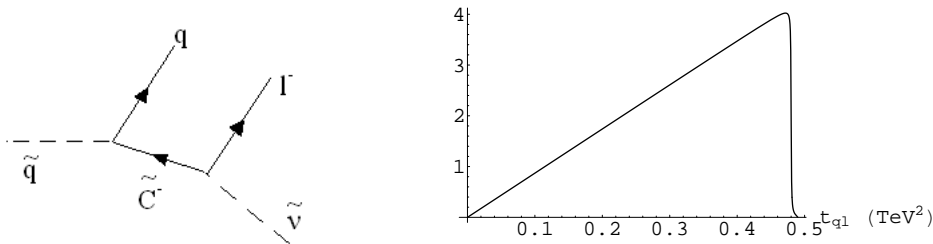


Figure 3: The decay of a squark through a chargino involves two chiral vertices. As a result the lepton’s direction is correlated with that of the outgoing quark. On the right we plot the amplitude as a function of t_{ql} for $m_{\tilde{q}} = 1000$ GeV, $m_{\tilde{C}} = 500$ GeV and $m_{\tilde{\nu}} = 300$ GeV. The graph is normalized to unit area.

because $m^2/q^2 \neq 1$, where q is the fermion 4-momenta (this possibility is also open to a Majorana fermion). This might become important if a decay must proceed through an off-shell particle simply because no other channel is available. We will not pursue this possibility further, but we comment on it in section (3.9).

The other possibility for a Dirac fermion to be polarized is when both its mother vertex and its daughter vertex are at least partially chiral. As an example, consider the decay of a squark into a quark, slepton and anti-lepton through a Chargino, as shown in figure (3). Using the rules we developed in the previous section it is straightforward to understand what angular correlations are expected.

In the rest frame of the Chargino, the decaying squark and outgoing quark define a polarization axis. Since the interaction is chiral the Chargino is polarized. Since the second vertex is also polarized, we have a polarized fermion decaying into another fermion (lepton) and a scalar (slepton). As we saw before, this decay is governed by a first order polynomial of $\cos \theta$. However, notice that $\cos \theta$ is related to the relativistically invariant quantity, t_{ql} ,

$$t_{ql} = (p_q + p_l)^2 = 2 \frac{(m_{\tilde{q}}^2 - m_{\tilde{C}}^2)(m_{\tilde{C}}^2 - m_l^2)}{4m_{\tilde{C}}^2} (1 - \cos \theta) \quad (3.1)$$

where the last equality only holds in the Chargino’s rest frame. We can immediately conclude that the relativistically invariant amplitude is at most a linear function of t_{ql} with the sign given by the explicit details of the couplings. Of course, this can be easily confirmed by an explicit computation of the amplitude, as shown in figure 3).

In contrast with the supersymmetric case let us consider the decay chain $q' \rightarrow q + W'^{\pm} \rightarrow q + W^{\pm} + \nu'$, where we have assumed that W' couples like a Standard Model W . The relevant diagram is shown in figure (4). If the spectrum is not too degenerate then in the rest frame of the W' , both the incoming q' and the outgoing q are boosted and mostly left-handed. Therefore, the W' longitudinal polarization dominates over the transverse one. Another way of seeing the same thing is to note that in the rest frame of W' the

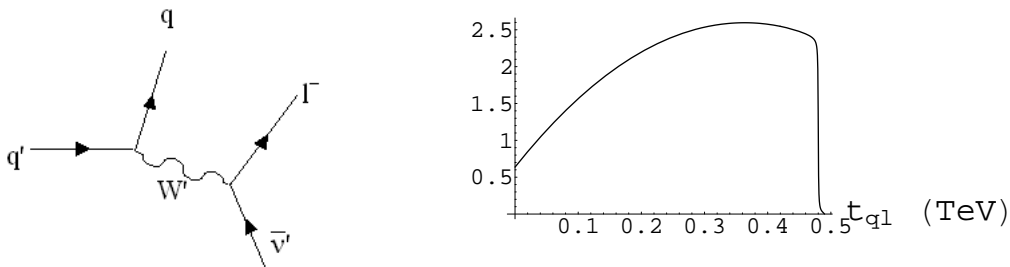


Figure 4: When q' decays the intermediate W' is longitudinally polarized if the incoming q' and outgoing q are both boosted in its rest frame. This in turn will result in angular correlations between the directions of the quark and the lepton. On the right we plot the amplitude as a function of $t_{q\ell}$ for $m_{q'} = 1000$ GeV, $m_{W'} = 500$ GeV and $m_{\nu'} = 300$ GeV. The graph is normalized to unit area.

fermionic current can be written in terms of the gauge-boson polarizations,

$$g_A \bar{u}_2 \gamma^\mu P_A u_1 \propto \left(\epsilon_{\text{long}} + \frac{m_{q'}}{E_{q'}} (c_L \epsilon_L + c_R \epsilon_R) \right) \quad (3.2)$$

where we have neglected m_q . c_L and c_R are $\mathcal{O}(1)$ coefficients depending on the precise nature of the interaction. Notice the suppression of the transverse polarization with respect to the longitudinal one by a factor of $m_{q'}/E_{q'}$ in the amplitude. It is clear that when the fermions' mass difference is comparable to the W' mass, $m_{q'} - m_q \sim m_{W'}$, the resulting polarization is negligible, since $m_{q'}/E_{q'} \sim 1$ in the rest frame of the W' .

Since the W' is longitudinally polarized, its subsequent decay into $l^+ \nu'$ is governed by a $1 - \cos^2 \theta$. Here, θ is the angle of the outgoing leptons with respect to the axis of polarization defined by the quarks. Therefore, the relativistically invariant amplitude squared must be a *quadratic* function of $t_{q\ell}$ with a negative coefficient in front of the leading power. Notice that a gauge-boson does not require the vertices to be chiral. This is important and potentially useful in determining the gluon partner's spin. However, it is also more susceptible to mass difference effects (see equation (3.2)). In contrast, the fermionic counterpart remains polarized even when $m_{\bar{q}}$ is not very different from $m_{\bar{c}}$, as long as the coupling is chiral and the outgoing quark is boosted.

Finally, we briefly consider the decay of the squark into $q\ell^\pm$ final states via a Majorana fermion intermediate state. The relevant diagrams are shown in figure (5). For the propagator to flip its spin we must place a mass insertion. However, due to the Majorana nature of the Neutralino, this corresponds to a different process with different final states than the one without a mass insertion. Therefore, the propagator has a definite helicity for each of the processes and there are angular correlations between the quark and the lepton. This fact was exploited by A. Barr [18] to determine the spin of the Neutralino and further details can be found in the reference. One can study $q\ell^+$ and $q\ell^-$ distributions to uncover the spin information. However, there is a further complication due the Majorana nature of the Neutralino. There is always another diagram starting from anti-squark with opposite

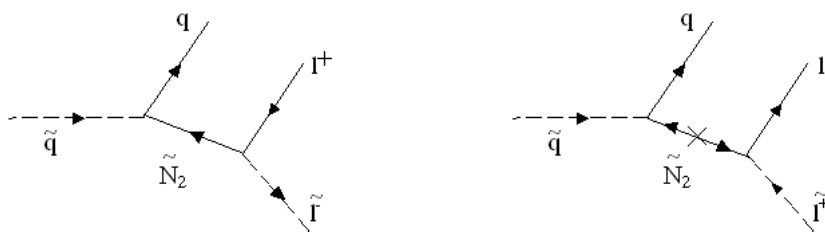


Figure 5: The two possible modes for a decay through a Neutralino. A spin flip requires a mass insertion (right), which results in a different process.

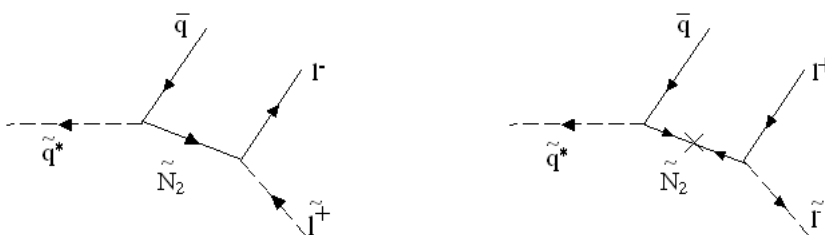


Figure 6: The two conjugate modes starting from an anti-squark for the decay through a Neutralino.

sign of its charge which contributes to the same process but with the opposite helicity structure as shown in figure (6). As Barr noted, in a proton-proton collider squarks and anti-squarks are produced unevenly and therefore the angular correlations are not washed out completely.

3.2 Weak decay with $q\bar{q}$ final states

In principle, the decay into $q\bar{q}$ final states could contain similar spin correlations, since it just replace the leptons in the second stage of the decay chains discussed in the previous section with quarks. However, in general we can not determine the charge of the initial jet. Once we are forced to average over the two final states shown in figure (5), all angular correlations are washed out.

On the other hand, if the decay products of the second decay are a third generation quark and quark partner we could, in principle, recover some charge information. It will then be possible to extract some spin correlation from such decay chains. The effectiveness of such decay channels require further careful studies taking into account the efficiency of identifying charge of the third generation quarks.

3.3 Weak decay with qW^\pm final state

If the charged gauge boson partner is lighter than the leptonic partner then its decay into a W^\pm and LSNP through a non-Abelian vertex is usually the dominant decay mode. This

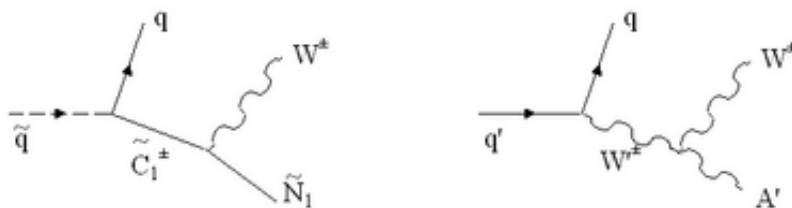


Figure 7: The weak cascade decay of a quark partner through the non-Abelian vertex in supersymmetry (left) and Same-Spin theories (right).

channel is shown in figure (7) In the supersymmetric case this coupling is at least partially chiral if $\tan\beta \neq 1$ and the higgsino is not considerably heavier than the gauginos. If $m_{\tilde{q}} - m_{\tilde{C}} \gg m_q$, then the chargino is at least partially polarized (with respect to the axis defined by the incoming squark and outgoing quark in its rest frame). In this case, since the chargino-neutralino- W coupling is also in general chiral, correlations between the quark and the outgoing W^\pm are present. The situation is a little more subtle than that since the contributions from a cascade initiated by an up-type partner cancel those initiated by a anti-down-type partner. However, due to the initial asymmetry between up quarks and anti-down quarks in the incoming PDFs the signal is not washed out. This decay exhibits a linear dependence on the variable $t_{qW} = (p_q + p_W)^2$.

The corresponding distribution for the Same Spin scenario is very different. In the rest frame of the W' both the incoming q' and the outgoing q are boosted and are mostly left-handed or mostly right handed. Hence the W' is longitudinally polarized. As a result, this decay exhibits a quadratic dependence on t_{qW} with a positive coefficient.

We will present a detailed study of this channel in section 4. At this point, we just remark that this is a more generic channel comparing with the channel requiring on-shell lepton partner in the decay chain. In fact, the existence this decay channel is based on a very minimal set of assumptions about the spectrum, in which only a heavy quark partner, a charged gauge boson partner and a LSNP are present. If the spectrum does not even allow for this decay chain, we will not be able to extract any information from weak decays. This appears to be the most promising channel.

3.4 Weak decay with qZ final state

There is a similar channel with a neutralino as the intermediate particle and a Z^0 in the final state (due to the higgsino-higgsino- Z^0 coupling). This could be a potentially golden channel considering the leptonic decay of the Z^0 . Unfortunately, there are no angular correlations since the $\tilde{N}_i \gamma_\mu P_\lambda \tilde{N}_j Z^\mu$ vertex is not even partially chiral. The Same-Spin counterpart is slightly ambiguous. If the intermediate particle is a heavy scalar partner of the higgs, there are no correlations. However, if the intermediate particle is some heavy Z' this might be the easiest channel to discover. As this is not a very generic case we will not pursue it any further.

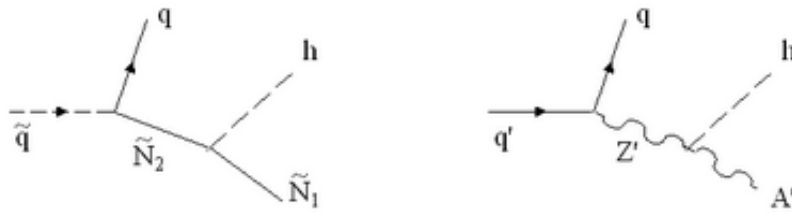


Figure 8: The weak cascade decay of a quark partner through a heavy neutralino into a higgs and LSP, in supersymmetry (left) and Same-Spin theories (right).

There is an additional complication concerning this process. When the Z^0 decays into quarks, this process is experimentally indistinguishable from the previous one we consider involving a W^\pm . However, in most models it is suppressed by a factor of 10 – 50 with respect to the chargino channel owing to the higgsino origin of the coupling. Therefore it does not present a serious background to it.

3.5 Weak decay with qh final state

The neutralino could also decay into a Higgs and LSP. This is shown in figure (8). In the supersymmetric case this process is possible because of mixing with the higgsino. Unfortunately, the $h\tilde{N}_1\tilde{N}_2$ vertex is not chiral and no correlation exists between the quark and higgs directions.

In the Same-Spin scenario this process is realized through the higgs coupling to the heavy gauge-bosons $g'vZ'_\mu A'^\mu h$. In this case, a correlation between the higgs and outgoing quark exists and follow the same as those for a massive gauge-boson decay into two bosons (the amplitude has a quadratic dependence on the variable t_{qh} with a positive coefficient).

This channel is quite generic and it is important to investigate it further. In certain cases, it might be possible to replace the outgoing quark with an outgoing lepton (for example heavy slepton production as discussed below in subsection 3.8). In a sense this is an orthogonal channel to that considered by Barr [18] as it relies on the existence of heavy leptonic partners rather than light ones.

3.6 Decay of gluon partner

In this section, we discuss the decay of the gluon partner into a quark and the quark partner. The quark partner subsequently decays into another quark and missing energy. This is shown in figure (9). This would certainly be the dominant channel of producing new physics particles if gluon partners are present in the spectrum. This diagram might prove to be the dominant decay mode into missing energy. Unfortunately, neither SUSY nor its Same-Spin counterpart have any spin effects present. The supersymmetric diagram certainly does not involve any correlations between the two outgoing jets owing to the scalar nature of the intermediate squark. In contrast the Same-Spin quark is indeed a fermion, however, its coupling to the gluon partner is vector like. Therefore, it is unpolarized and

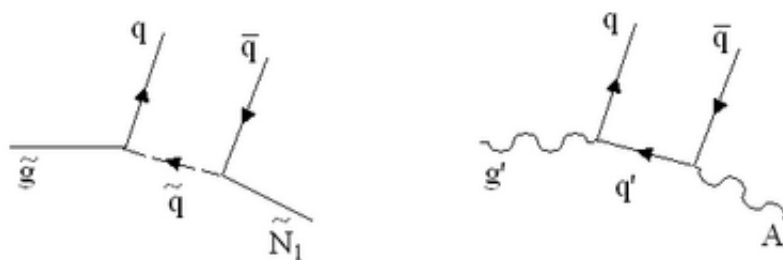


Figure 9: The cascade decay of the gluon partner in supersymmetry (left) and Same-Spin theories (right).

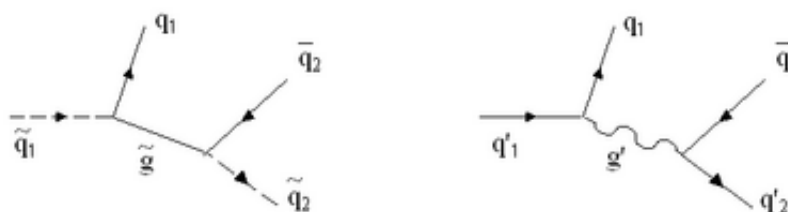


Figure 10: The strong cascade decay of a heavy quark partner in supersymmetry (left) and Same-Spin theories (right).

its subsequent decay is isotropic. In the present work we will not consider this channel any further, leaving a detailed study to a future publication.

If the spectrum is such that the gluon partner must decay into the LNSP via an off-shell quark the situation is quite different. We discuss this issue further in subsection 3.9.

3.7 Strong decay of quark partner

Next we consider the strong decay of a quark partner. This scenario is slightly specialized as it relies on the existence of a squark heavier than the gluino, but it is still generic enough to warrant consideration. The relevant diagram is shown in figure (10). If such a quark partner indeed exist this will be its dominant decay mode. The supersymmetric case still has no angular correlations between the outgoing jets owing to our experimental limitations. As discussed above, the Majorana nature of the gluino makes it possible to observe correlations without having chiral vertices. There are two diagrams, one with a mass insertion and the other without. The former involves two outgoing quarks and the latter a quark and an antiquark. Unfortunately, all that we observe in the lab are two jets and must average over the two contributions. Therefore the decay should have no dependence on the variable $t_{q_1 q_2} = (p_{q_1} + p_{q_2})^2$.

The Same-Spin case, however, does possess angular correlations between the outgoing jets and is distinguishable from the supersymmetric one. As discussed above, the Same-

Spin gluon is longitudinally polarized and we expect the decay to be a quadratic function of the variable $t_{q_1 q_2}$. The biggest challenge such a measurement faces is the significant background due to Standard Model processes. This may not be an insurmountable impasse. The subsequent decay of q' together with hard cuts on missing energy might reduce the background dramatically. This is an important enough channel with a clear enough signature (if isolated) to warrant further study which we hope to address in a future publication.

Notice that the second stage of the decay chain could involve third generation quarks and squarks. In this case, since we might recover some charge information, this decay can be useful to determine the spin of the gluino. It is not uncommon that the third generation squarks are lighter than the first two generation squarks. In particular, RGE running and a large third generation Yukawa coupling usually results in a lighter third generation squarks. Therefore, if $m_{\tilde{q}_3} \geq M_{\tilde{g}}$ or just slightly lighter, and $m_{\tilde{q}_{1,2}} > m_{\tilde{q}_3}$ there could be a significant enhancement of branching ratio into third generation quark and quark partners. Even in the Same Spin scenario, decaying into third generation quark and quark partner could help reduce the combinatorial background.

As mentioned above, in the case of left-right asymmetric spectrum, the two vertexes are effectively chiral and that will effect the angular correlations.

3.8 Decay from leptonic initial states

Many of the channels discussed above, involved the weak decay of a quark partner. If lepton partners are heavy enough, all such channels can be initiated by a lepton partner decay instead. The angular correlations are the same, only we replace an outgoing jet with an outgoing lepton. Such a scenario can be realized through the Drell-Yan production of heavy lepton partners.

Such a cascade has several advantages. First, jet combinatorics is not a problem. Second, we gain a lot more information because charge and flavor is now available to us. This is extremely helpful. For example, in the weak decay with l, W^\pm final state, there is only one channel to consider and no averaging is needed.

On the other hand, a lepton partner at the beginning of a cascade is harder to come by. It could come from the decay of heavy electroweak gauge boson partner, or a Z' coupled to leptons. But, that is more model dependent. We also require there to be several states below the lepton partner. This could sometimes require special arrangements. For example, in the MSSM, we would require a mass hierarchy such as $M_2 > m_{\tilde{\ell}} > M_1 > \mu$. This avenue looks promising in certain regions of parameter space.

3.9 Off-shell decays

So far, we have only considered on-shell decay processes. We saw that if the intermediate particle is a Dirac fermion the interactions involved must be at least partially chiral. This conclusion is modified if that particle is off-shell. Although on-shell decays usually dominate, there are special kinematical regions where we are forced to have off-shell decays. For example:

1. If the quark partner is heavier than the gluon partner, gluon partner will be forced to decay through an off-shell quark partner.

2. The decay of a gauge boson partner to LNSP will be forced to go through an off-shell W/Z and lepton/quark partners if the mass splitting is small. The virtual lepton-partner and virtual quark channels could be particularly interesting since it brings in new spin information about the lepton partner. It could be important over a large mass range of the lepton partner since the decay to off-shell W/Z is usually suppressed by mixing.

To illustrate this point we consider the first example where the gluon partner decays through an off-shell quark partner. The relevant diagrams are shown in figure (9). The SUSY channel obviously has no correlations since the squark is a scalar. However, in the Same-Spin scenario correlations are present. The amplitude for this process is

$$\sum_{\text{pol}} |\mathcal{M}|^2 \propto 2 \frac{(m_{q'}^2 - q^2)(q^2 - 2m_{g'}^2)(q^2 - 2m_{A'}^2)}{m_{g'}^2 m_{A'}^2} t_{q\bar{q}} + f_0(q^2), \quad (3.3)$$

where we neglected the trivial denominator. $f_0(q^2)$ is some complicated function of q^2 , the momentum of the internal quark partner, and the masses. It is irrelevant for this discussion. Notice that when the quark partner is off-shell $q^2 \neq m_{q'}^2$ and the coefficient of $t_{q\bar{q}} = (p_q + p_{\bar{q}})^2$ is non-zero. This linear dependence of the cross-section on $t_{q\bar{q}}$ can in principle be distinguished from the SUSY case where there is no dependence on $t_{q\bar{q}}$. Further study is needed to explore the observability of this effect in different models.

Similar considerations apply for the other case of a gauge-boson partner decay to LNSP via an off-shell slepton.

4. Determining spin without leptonic partners

In this section we will explore the decay of a quark partner into a charged weak partner which consequently decays into a W^\pm and missing energy. Let's begin with the supersymmetric case. The squark-quark-chargino vertex is given by [31] (we are ignoring the CKM and super-CKM matrices as they are quite irrelevant to the following discussion),

$$\mathcal{L}_{q\bar{q}\tilde{C}^+} = -g_2 \left(\bar{u} P_R (U_{11} \tilde{C}_1 + U_{21} \tilde{C}_2) \tilde{d} + \bar{d} P_R (V_{11} \tilde{C}_1^c + V_{21} \tilde{C}_2^c) \tilde{u} \right) \quad (4.1)$$

where U_{ij}, V_{ij} are the matrices diagonalizing the Chargino's' mass matrix. We are assuming that the chargino is dominantly a gaugino and ignore the direct quark-squark-higgsino couplings. The more important vertex is the chargino- W^+ -neutralino coupling,

$$\mathcal{L}_{W^-\tilde{C}\tilde{N}} = g_2 W_\mu^- \tilde{N}_i \gamma^\mu (O_{ij}^L P_L + O_{ij}^R P_R) \tilde{C}_j \quad (4.2)$$

where,

$$\begin{aligned} O_{ij}^L &= -\frac{1}{\sqrt{2}} N_{i4} V_{j2}^* + N_{i2} V_{j1}^* \\ O_{ij}^R &= \frac{1}{\sqrt{2}} N_{i3}^* U_{j2} + N_{i2}^* U_{j1} \end{aligned} \quad (4.3)$$

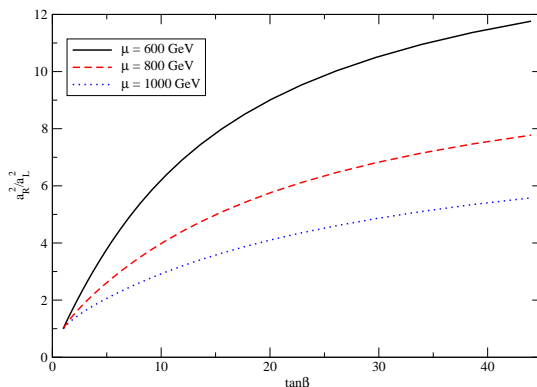


Figure 11: The ratio of the right to left couplings a_R^2/a_L^2 as a function of $\tan\beta$ for three different values of the μ -parameter. $M_1 = 100$ GeV and $M_2 = 500$ GeV are fixed.

and N_{ij} are the mixing matrices for the Neutralino. This interaction is usually at least partially chiral (when $\tan\beta \neq 1$). Therefore we expect the amplitude to have some $t_{qW} = (p_q + p_W)^2$ dependence, with a coefficient given by the difference of the couplings in equation (4.3). Indeed, in the narrow width approximation $q^2 \rightarrow m_{\tilde{C}}^2$ we get,

$$|\mathcal{M}|^2 \propto \frac{1}{2} \left(\frac{m_{\tilde{C}}^2(m_{\tilde{C}}^2 - m_{\tilde{N}}^2 - 2m_W^2)}{m_W^2} \right) (a_L^2 - a_R^2) t_{qW} + f_0(q^2, m_i) \quad (4.4)$$

where $f_0(S, m_i)$ is a polynomial given in the appendix. The 3-body phase-space differential volume can be written in terms of q^2 and t_{qW} (see for example [32]),

$$dPS_3 = \frac{1}{128\pi^3 m_1^2} dq^2 dt_{qW} \quad (4.5)$$

with appropriate kinematic boundaries. In the narrow-width approximation the integration over q^2 is trivial and simply removes the denominator in equation (4.4) and replaces $q^2 \rightarrow m_{\tilde{C}}^2$. Therefore, the angular correlations in this decay depend on the difference $(a_L^2 - a_R^2)$.

In figure (11) we plot the ratio a_R^2/a_L^2 as a function of $\tan\beta$ for a few values of μ -parameter with $M_1 = 100$ GeV and $M_2 = 500$ GeV. This ratio is quite different than unity for most choices of the parameters.

There is one additional complication in the SUSY case. As seen from equation (4.1) there are two contributions to any process involving the chargino. One comes from the coupling to the up squark, while the other comes from the coupling to the anti-down squark. Therefore, as shown in details in the appendix these two contributions differ by the sign of the coefficient of t_{qW} . Since we cannot distinguish between a jet coming from a down quark and that coming from an anti-up quark, we must average over the two contributions. Fortunately, due to the composition of the proton there are more up-like squarks produced

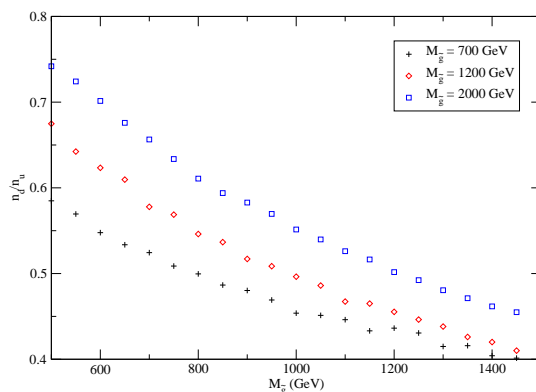


Figure 12: The ratio of down squarks to up squarks in production as a function of their mass for different gluino masses, $m_{\tilde{g}} = 700, 1200, 2000$ GeV (black-solid, red-dashed, green-points).

than down-like squarks. Their ratio in production is shown in figure (12) as a function of their mass and gluino mass.

Let us contrast this with the corresponding process in Same-Spin theories. The intermediate particle is a spin-1 Same-Spin W^\pm . As we argued before in equation (3.2) it is dominated by the longitudinal mode. Therefore its subsequent decay is dominated by the angular distribution of the second equation in (2.5). Therefore the W^+ boson is preferentially collinear or anti-collinear with the jet. We expect $a_2(t_{qW})^2 + a_1 t_{qW} + a_0$ dependence with $a_2 > 0$ and $a_1 \leq 0$. The computation is quite involved, but the final expression is indeed,

$$|\mathcal{M}|^2 = \frac{1}{(q^2 - M^2)^2} (F_0(q^2, m_i) + F_1(q^2, m_i)t_{qW} + F_2(q^2, m_i)(t_{qW})^2) \quad (4.6)$$

where the F_i 's are given in the appendix. It is not hard to show that $F_2(M^2, m_i) > 0$ and $F_1(M^2, m_i) < 0$. The shape of the resulting cross-section is plotted in figure (13) against the corresponding SUSY cross-section. The behavior for small t_{qW} is distinctly different than the supersymmetric case. The reason is clear. Small values of t_{qW} corresponds to W^+ being collinear with the jet, which is forbidden in the supersymmetric process, but preferred in the Same-Spin case. We have also included in figure (13) the results of the Monte-Carlo simulation.

4.1 Experimental observable - lepton-jet correlation

Of course, we have to take into account the fact that W^+ cannot be observed directly and only its decay products can be measured. If it decays to quarks and it is possible to distinguish these two jets from the rest by reconstructing the W^+ (as it is on-shell) the signal might still be very strong. We include standard cuts to reduce Standard Model background. We also consider the contribution from other new physics processes with identical

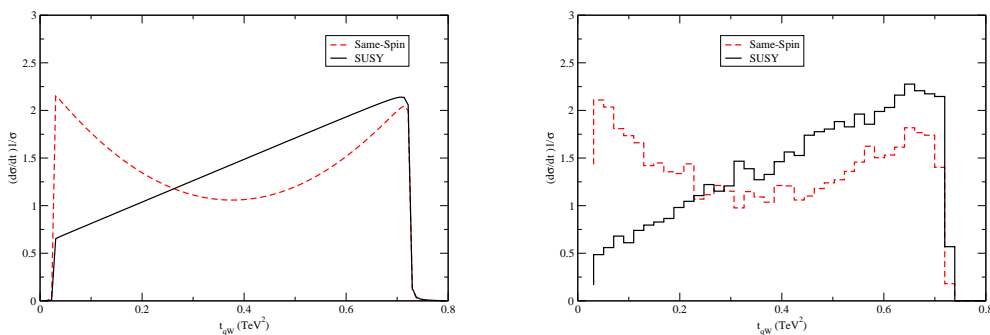


Figure 13: Theoretical curves (Left graph) for the q-W correlations in the two models (solid,black - SUSY, dashed,red - Same-Spin). Cross-section is plotted against the t_{ql} variable. The right plot shows the Monte-Carlo simulation. Both graphs are normalized to unit area.

final states. We argue that this signal is still a strong candidate for spin determination.⁵ In this subsection, however, we concentrate on the other option, namely, the leptonic decay of the W^\pm . The main challenge we face is that we cannot reconstruct the W^+ as the neutrino is unobservable. To investigate the resulting signal we used the Monte-Carlo event generator HERWIG [24]. We implemented spin-correlations for massive spin-1 particles and the details can be found in appendix B. For the Same-Spin production matrix elements we used the ones quoted in [20].⁶

We expect much of the difference to be washed out once the W^+ is allowed to decay into leptons. The only observables we are left with are the momenta of the outgoing jet and that of the lepton. Therefore, we will plot the cross-section as a function of the invariant mass $t_{ql} = (p_q + p_l)^2$. Figure (14) shows the Monte-Carlo simulation results when the lepton is correlated with the jet from its own branch. In practice we have no way to tell which jet came from which branch and we amend this below.

While the behavior is indistinguishable at high t_{ql} , it is certainly very different at low t_{ql} . We can attribute this to the fact that in the SUSY model, the W^+ is very unlikely to be collinear with the jet, whereas the opposite is true for the Same-Spin model.

This plot suggests that the two models are still distinguishable from one another even if the W cannot be fully reconstructed. When taking into account the jet combinatorics by pairing the lepton with both jets in the event the results do alter. In figure (15) we plot the cross-section against t_{ql} for events with two jets and one or two leptons (the two-leptons

⁵A detailed study of Standard Model background with sophisticated jet analysis is beyond the scope of this paper. We will begin to address this issue in future publications.

⁶Except for the matrix element $\mathcal{M}(qq \rightarrow q_1^* q_1^*)$ which was taken from [33] since the one quoted in [20] seemed to give production rates which are too large. Strictly speaking, those are inappropriate for the model we consider (as they assume degenerate spectrum and only one mass scale, namely $1/R$, the compactification radius). However, nothing in our discussion seems to rely heavily on the precise production cross-section and we do not expect any major modification to the conclusions below. To simplify the analysis we switched off cluster formation, heavy hadron decays and the underlying soft event.

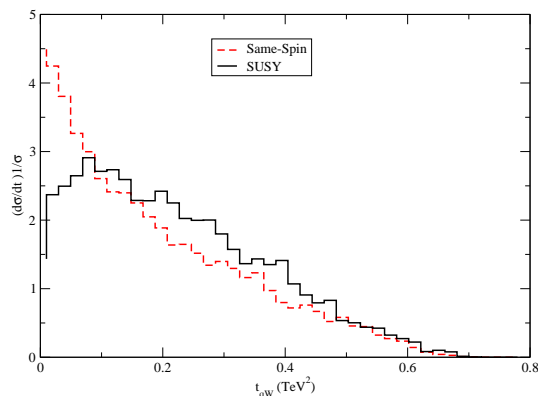


Figure 14: Monte-Carlo simulation for the quark-lepton correlations in the two models (solid,black - SUSY, dashed,red - Same-Spin). Normalized cross-section is plotted against the t_{ql} variable. The data sets contain $\sim 13,000$ events each.

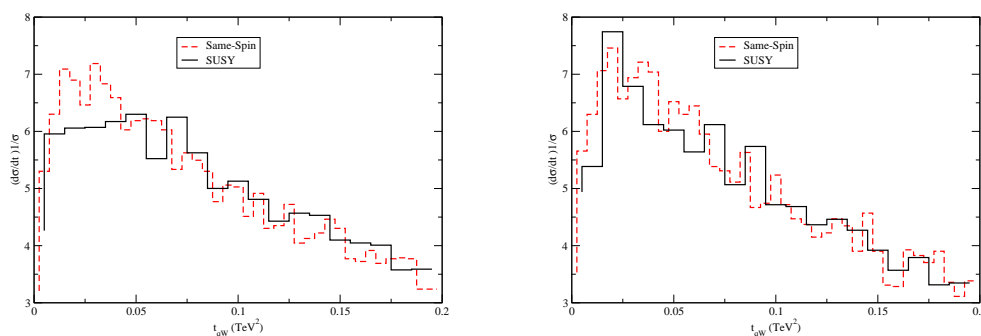


Figure 15: Monte-Carlo simulation for the jet-lepton correlations in the two models (solid,black - SUSY, dashed,red - Same-Spin) with no knowledge of the correct pairing. Normalized cross-section is plotted against the t_{ql} variable. The graph on the left is for 2 jets and 1 lepton events. The graph on the right corresponds to 2 jets 2 opposite sign leptons events. The data sets contain $\sim 17,000$ events with 1 lepton and $\sim 9,000$ events with 2 leptons for each of the models.

case corresponds to both branches decaying into a lepton). The single lepton diagram still exhibits the flattening of the cross-section in the SUSY case for low t_{ql} . This is in contrast with the rising cross-section for the Same-Spin model. It is possible that close analysis of low t_{ql} can pick up this difference once real data is available. There is no obviously observable spin dependence in the second case with two leptons in the final state.

4.2 Experimental observable - jet- W correlation

In this section we take up the second possibility, namely that the W^\pm decays into two jets. The advantage is the ability of fully reconstructing the four momenta of the W^\pm 's. There

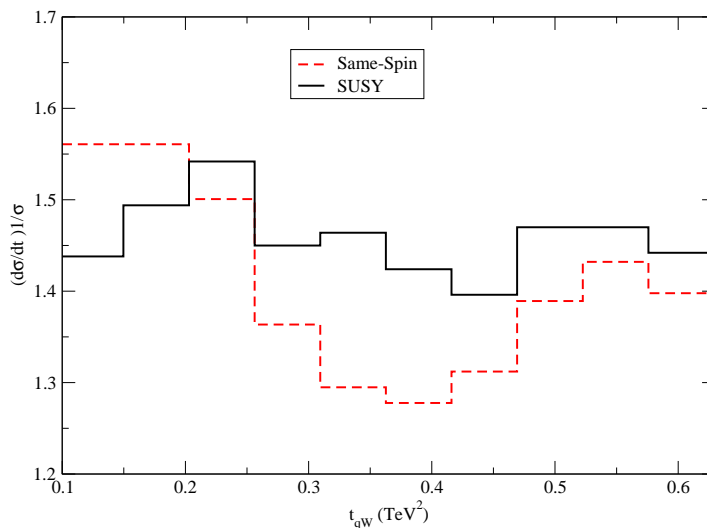


Figure 16: Considering only 4-jet events this is a histogram of the invariant mass t_{W,j_i} for each of the models: SUSY (solid-black), Same-Spin (dashed-red). The histogram is normalized to unit area. The two data sets contained $\sim 9,000$ and $2,000$ events, respectively. The normalized error is approximately $\sqrt{N} \sim 0.04$.

are disadvantages as well. First and foremost, very naively the Standard Model background is significant. Second, since jets are involved, momentum determination involves some amount of smearing. This would affect the reconstruction of W^\pm as well as the angular correlations. Third, it is very hard to distinguish between a W^\pm and a Z^0 and so when investigating background we must consider both. We do not attempt a full Standard Model background analysis, however, there are several reasons why it might be possible to reduce such a background. First, hard cuts on missing energy can yield a fairly clean sample of beyond the standard model physics. Second, we can easily have additional leptons in the process we consider. Simply let the quark partner in the other branch (shown in figure (17)) to decay into a Z' or W' . It is not hard to imagine other possible channels for producing leptons in the final state. The problem of background reduction is beyond the scope of this paper and we will assume that some non-negligible set of events, containing new physics, can be isolated and analyzed.

We consider 4-jet events with a typical event topology shown in figure (17) together with a possible background from another new physics process. In every event we try to reconstruct the W^\pm from two of the 4 jets and then form the invariant mass t_{qW} with the two remaining jets. If more than one pairing reconstructs W it is regarded as failure and the event is discarded. Our cuts involve $\cancel{P}_T > 200$ GeV and $\eta < 4.0$. We make no attempt in trying to order the jets by the magnitude of their transverse momentum or some more sophisticated ordering (This very naive approach yields a significant difference between the

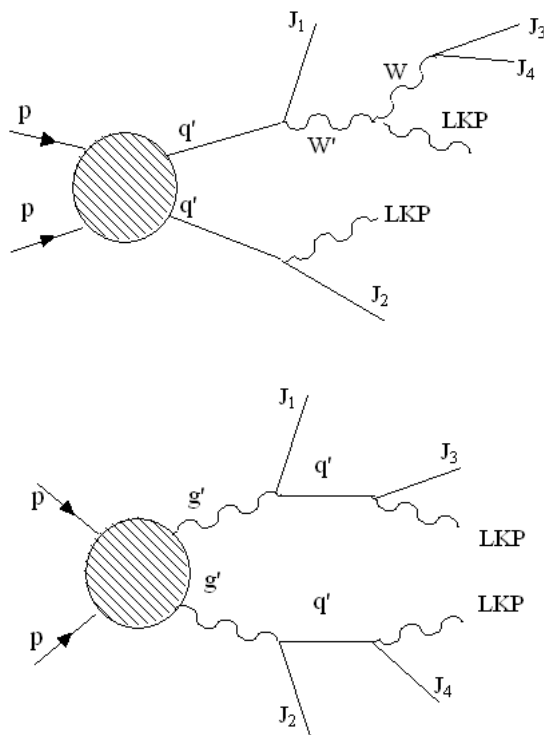


Figure 17: 4-jet event topology for the Same-Spin theory. The diagram we are interested in (left) together with a possible Same-Spin irreducible background (right)

two models as shown in figure (16)). There can certainly be potential improvements on this measurement by using more kinematical information of the jets. The linear behavior vs. the the quadratic behavior is still visible on top of the background coming from the wrong pairing.

There could also be background from different processes in the same model of new physics with identical final states. One such channel is shown on the right in figure (17) for Same-Spin theory and figure (18) for the SUSY case. We consider all events with 4-jets. Then we construct the invariant mass $m_{j_k, j_l}^2 = (p_k + p_l)^2$ for every possible pair. We used HERWIG internal algorithm for jet progenitor formation.⁷ We include jet smearing effects [34] using the ATLAS specs [5]. The results are shown in figure (19). The irreducible background does not seem to pose a serious concern as the W peak is clearly visible. This should come as no surprise. With a random pairing of such energetic jets, the chance of reconstructing a quantity with < 100 GeV is fairly low. This can probably be made even sharper with some simple cuts on jet energy. For example, the initial jets from the squark decay tend to be more energetic than those coming from the W .

The above discussion is by no means a proof that the reconstruction of the W is an easy task. It merely serves to show that it is not hopeless and to encourage further study

⁷This object is not a jet, but would become one after a proper experimental jet algorithm is applied.

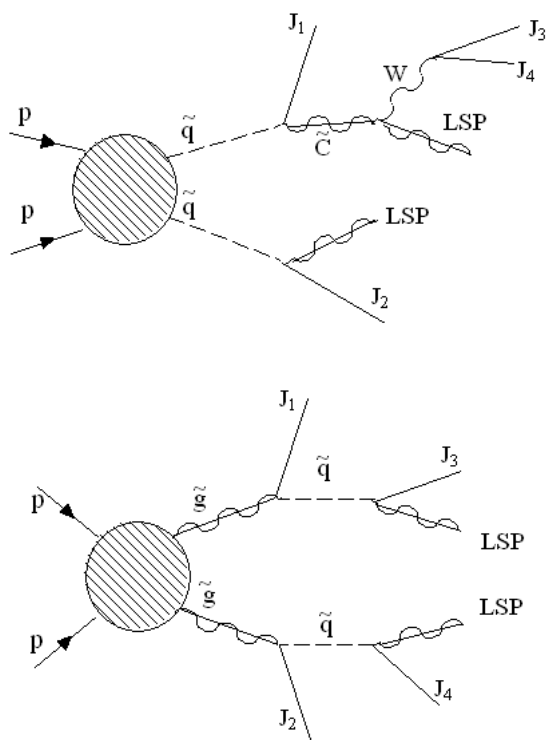


Figure 18: 4-jet event topology for SUSY. The diagram we are interested in (left) together with a possible SUSY irreducible background (right)

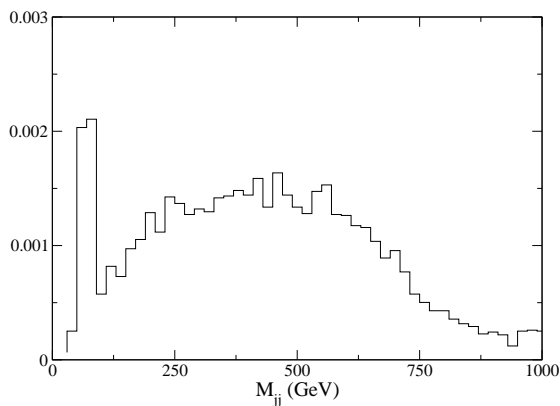


Figure 19: Considering only 4-jet events we plot a histogram of the invariant mass $m_{j_k, j_l}^2 = (p_k + p_l)^2$ of all possible pairs of jets. The graph is normalized to unit area.

of this possibility involving a proper detector simulator and a more detailed analysis of the background.

4.3 Scanning M_1 and M_2

It is important to map out the regions of parameter space in which the different channels are useful. In this section we present the results of a scan covering the subspace spanned by (M_1, M_2) . We also set $m_{W'} = M_2$ and $m_{A'} = M_1$. While there are other parameters which effect the results (such as $\tan\beta$, $m_{\tilde{q}}$, μ , etc.) we focus on those two parameters, (M_1, M_2) , which are the most determinantal to the observability of angular correlations for the channel we consider.

When performing such a scan, we wish to assign a number to quantify the difference between, say, the distribution describing the SUSY scenario and that of the Same-Spin scenario. There is no unique choice for such a number. Moreover, such an assignment can be problematic as it can overlook differences that a more careful analysis would pick up. Therefore, the results of this section should be understood with the following proviso in mind: the numbers assigned for the different points in parameter space carry only relative importance among themselves and have very little absolute meaning. They indicate that in certain regions spin determination is easier as compared with other regions.

There is one more point to keep in mind. We will compare the distributions produced for the two models by matching their spectrum. This is incorrect. One should match the cross-section first as that is the actual experimental observable. Unfortunately, we had poor control over the production rates for the Same-Spin scenario.⁸ However, this is not entirely misleading. As part of our results we will consider the observability of each of the models against phase-space. Therefore, if nothing else, we are able to tell when spin effects are present at all.

To quantify the difference between the distributions we use the Kolmogorov-Smirnov test for goodness-of-fit. In this test, the cumulative distribution functions (CDF) of both data sets are compared. The D-statistics is simply the maximum vertical difference between the CDF's. In other words,

$$D = \sup |F_1(x) - F_2(x)| \quad (4.7)$$

where $F_1(x)$ and $F_2(x)$ are the CDF's for the two data sets. The p-value assigned to the D-statistics is low when the two data sets come from different underlying distributions. There are several advantages to the Kolmogorov-Smirnov test. First, it is a non-parametric test so it applies to general distributions. Second, it is independent of the way we choose to histogram the data.

In figure (20) we plot the p-value as a function of M_2 for three different values of M_1 . The quark partner mass is $m_{\tilde{q},q'} = 1000$ GeV, the gluon partner mass is $m_{\tilde{g},g'} = 1200$ GeV. We set $\tan\beta = 10$ in the supersymmetric case. For every value of the parameters we produced 100,000 events out of which only about 10% passed the different cuts.

The scan matches our expectations. When $M_2 \rightarrow M_1$ the LSP and the W are produced at rest and there the correlations with the polarization axis defined by the quark partner are diminished. Also, when $M_2 \rightarrow m_{\tilde{q},q'}$ it becomes harder to distinguish the two data

⁸The production cross-sections given in [20] for the Same-Spin theory have only one adjustable parameter, namely the inverse compactification radius.

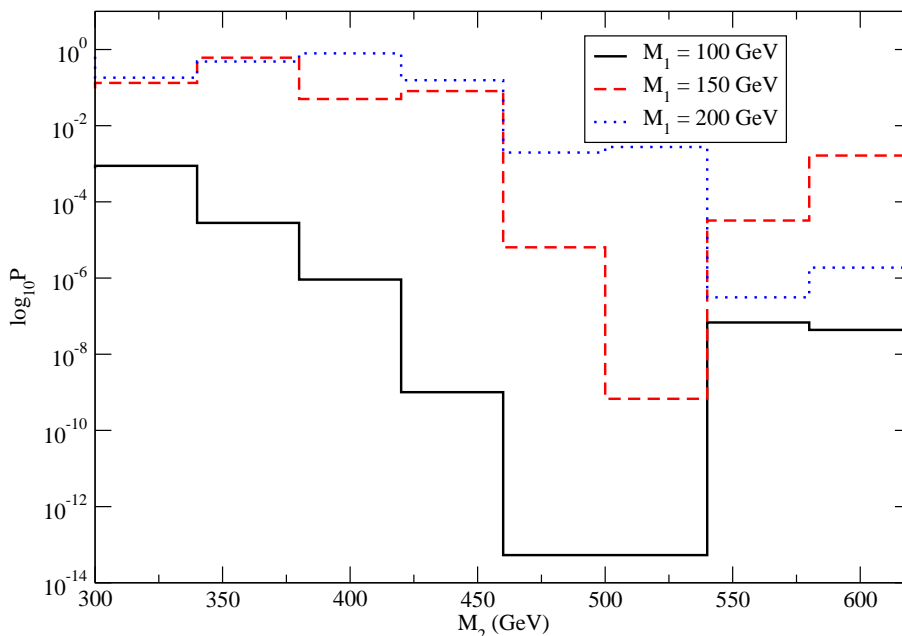


Figure 20: A plot of the p-value vs M_2 for different values of M_1 . We set $m_{W'} = M_2$ and $m_{A'} = M_1$. The p-value is lower when the two data sets are more distinguishable. The other parameters were fixed at $m_{\tilde{q},q'} = 1000$ GeV, $m_{\tilde{g},g'} = 1200$ GeV. We set $\tan\beta = 10$ in the supersymmetric case. Both data sets contained $\sim 10,000$ events. Notice that when the mass splitting between M_1 and M_2 is small, i.e. the left-hand side of the plot, it is harder to distinguish these two scenarios. Supersymmetry and Same-Spin scenario become more distinguishable as the mass splitting increases. However, as M_2 approaches $m_{\tilde{q},q'}$ the difference is again diminished.

sets. This is also expected because in the Same-Spin case the quark partner, q' , is not at all boosted in the rest frame of the W' . Therefore, W' is not polarized.

The results are encouraging. While a more sophisticated analysis (better cuts, better fitting, more realistic collider simulation, etc.) is certainly warranted, these initial results seem to indicate that spin determination is possible. As pointed out before, one should not confine the analysis to special benchmark points, but rather attempt a scan over the parameter space. In this way, an inclusive strategy, combining several channels, can be devised to cover different exclusive regions of the parameter space.

5. Conclusions and future directions

We have systematically studied the possibility of measuring the spin of new particles in a variety of cascade decays. Generally, the existence of a LNSP renders the reconstruction of the momenta of new physics particles impossible. Therefore, we focused on distributions

of relativistically invariant variables. We identified a set of decay channels which are useful for spin determination.

A general lesson of this study is that even though spin correlations are present in a variety of decay channels, the viability of any particular channel is always confined to certain kinematical regions. As a result, different models of new physics with different spectra tend to give very different useful channels for spin determination. Different strategies will have to be employed at the LHC. Therefore, we emphasize that it is important not to confine ourselves to any particular benchmark model or any particular decay mode. We should instead explore the effective range of all possible decay channels and devise techniques for using them efficiently. In this sense, our survey of potentially useful decay channels is the initial step of an important task for which many detailed studies still need to be done.

As part of this program we studied the decay channel $\tilde{q} \rightarrow q + \tilde{C}^\pm \rightarrow q + W^\pm + LSP$. A scan over the chargino and neutralino masses was performed. We found that as long as the spectrum is not too degenerate the prospects for spin determination are rather good.

One of the most important challenges is to measure the spin of gluon partners. The difficulty in such a study is that the decay products carrying the spin information of the gluon partner are usually jets, missing the charge information. In addition, such channels usually have larger combinatorial background and Standard Model background. A similarly challenging task is a direct measurement of the spin of the quark partner.

We have considered only kinematical variables constructed out of two objects of the decay products. It is in principle interesting to study the possibility of using more complicated kinematical variables.

Notice that decay channels involving leptons are generally more promising than those involving only jets. This result stems from the fact that we have charge and flavor information from the lepton, which could help us in separating the channels. We have assumed no such information from jets. Therefore, we have limited information from channels decaying into quarks, except for the third generation. Moreover, losing charge and flavor information from the jet significantly increases the combinatorial background, since typical new physics signals for the scenarios considered in this paper almost always contain several hard jets. Therefore, any potential information about the charge and flavor of the initial parton of the jet will be very helpful in spin determination.

We would like to remark that reducing combinatorial background is very important in extracting more information about the underlying new physics. This led the authors of [9] to conclude that to what extent jet charge could be measured is an important study for LHC experiments.

We have not studied the possibility of measuring spin in the production. This is certainly a very important area to be investigated carefully. Barr [30] has studied the measurement of the spin of muon partners using angular distribution from pair production. In principle, angular distributions of production of other partners should carry similar information. This is a subject currently under investigation. One of the main complications is the existence of t-channel productions. Such production channels bring in more partial-waves and tend to wash out characteristic angular distributions.

We would also like to emphasize that although we have only compared SUSY with the Same-spin scenario, the general rules we have developed in the paper are easily applicable to any generic scenario with different spin content of new physics particles.

Acknowledgments

We would like to thank the following people for useful discussions: Nima Arkani-Hamed, Michael Peskin, Gui-Yu Huang, Jesse Thaler and especially Tao Han whose encouragement and suggestions were very helpful.

A. Matrix elements calculations

In this appendix we present the explicit matrix elements for the decays considered in the text. We begin with the Same-Spin decay channel $q' \rightarrow q + W' \rightarrow q + W + A'$. The matrix element is given by,

$$\begin{aligned}
 i\mathcal{M} = & \quad \begin{array}{c} q \\ \nearrow p_2 \\ \text{---} p_1 \text{---} \\ \text{---} W' \text{---} \\ \searrow p_3 \text{---} W \\ \text{---} p_4 \text{---} A' \end{array} \\
 = & \quad g_2 \bar{u}(p_2) \gamma_\mu P_L u(p_1) \frac{i}{q^2 - m_{W'}^2} \left(-g^{\mu\nu} + \frac{q^\mu q^\nu}{m_{W'}^2} \right) \\
 & \quad \times e (g_{\rho\nu} (-q - p_3)_\sigma + g_{\nu\sigma} (p_4 + q)_\rho + g_{\sigma\rho} (p_3 - p_4)_\nu) \epsilon^\sigma(p_4) \epsilon^\rho(p_3)
 \end{aligned}$$

We have borrowed the usual Standard Model coupling for the vertices. The probability amplitude is then,

$$\sum_{pol} |\mathcal{M}|^2 = c_2 (t_{qW})^2 + c_1 t_{qW} + c_0$$

Where the coefficient functions are,

$$\begin{aligned}
 c_2 = & \quad \frac{1}{(q^2 - m_{W'}^2)^2} \frac{m_W^4 + (m_{A'}^2 - q^2)^2 + 2m_W^2(5m_{A'}^2 - q^2)}{m_W^2 m_{A'}^2} \\
 c_1 = & \quad \frac{1}{(q^2 - m_{W'}^2)^2} \frac{1}{m_{W'}^2 m_{A'}^2 m_W^2} \\
 & \quad \times \left(-(m_{q'}^2 - m_q^2)(m_W^2 - m_{A'}^2)(m_{A'}^4 + 10m_W^2 m_{A'}^2 + m_{A'}^4 - q^4) \right. \\
 & \quad + m_{W'}^2 (-m_W^6 - 11m_W^4 m_{A'}^2 - 11m_W^2 m_{A'}^4 - m_{A'}^6 + 3m_W^4 q^2 \\
 & \quad + 14m_W^2 m_{A'}^2 q^2 + 3m_{A'}^4 q^2 - 3m_W^2 q^4 - 3m_{A'}^2 q^4 + q^6 \\
 & \quad + m_{q'}^2 (m_W^4 - 10m_W^2 m_{A'}^2 - 3m_{A'}^4 + 4m_{A'}^2 S - q^4)) \\
 & \quad \left. + (m_q^2 (-3m_W^4 + m_{A'}^4 - q^4 + m_W^2 (-10m_{A'}^2 + 4q^2))) \right)
 \end{aligned}$$

The last term, c_0 is too complicated to present and carries little significance. It is not hard to show that c_2 is always positive for any real choice of q^2 .

Next we are interested in the corresponding SUSY decay chain shown in figure (21). The first vertex is given by,

$$-g_2 V_{11} \bar{d} P_R \tilde{C}^c \tilde{u} \quad \text{and} \quad -g_2 U_{11}^* \bar{\tilde{C}} P_L u \tilde{d}^* \quad (\text{A.1})$$

respectively. The $\tilde{N}\tilde{C}W^+$ vertex is given by,

$$g_2 W_\mu^- \tilde{N}_i \gamma^\mu (\mathcal{O}_{ij}^L P_L + \mathcal{O}_{ij}^R P_R) \tilde{C}_j \quad (\text{A.2})$$

The matrix element for the decay initiated by a down-type squark is,

$$\mathcal{M}_{\tilde{d}} = g_2^2 U_{11}^* \bar{u}_{\tilde{N}}(p_4) \gamma^\mu (\mathcal{O}_{11}^L P_L + \mathcal{O}_{11}^R P_R) \frac{\not{q} + M_{\tilde{C}}}{q^2 - M_{\tilde{C}}^2} P_L v_u(p_2) \epsilon_\mu(p_3) \quad (\text{A.3})$$

$$= U_{11}^* \bar{u}_{\tilde{N}}(p_4) \gamma^\mu \frac{a\not{q} + bM_{\tilde{C}}}{q^2 - M_{\tilde{C}}^2} v_u(p_2) \epsilon_\mu(p_3) \quad (\text{A.4})$$

where,

$$a = g_2^2 \mathcal{O}_{11}^R \quad \text{and} \quad b = g_2^2 \mathcal{O}_{11}^L \quad (\text{A.5})$$

The squared amplitude is given by,

$$|\mathcal{M}_{\tilde{d}}|^2 = \frac{(b^2 m_{\tilde{C}}^2 - a^2 q^2)(q^2 - 2m_W^2 + m_{\tilde{N}}^2)}{2m_W^2(q^2 - m_{\tilde{C}}^2)^2} t_{qW} + \text{Const.} \quad (\text{A.6})$$

Therefore, in the narrow width limit, the slope depends on the difference $b^2 - a^2$. The problem is that the second diagram contributing to this process (with an up-squark decay) has the opposite sign for this coefficient. Notice that,

$$\begin{aligned} \bar{d} P_R \tilde{C}^c \tilde{u} &= -(\tilde{C}^c)^T P_R \bar{d}^T \tilde{u} = -\bar{\tilde{C}} C^T P_R \bar{d}^T \tilde{u} \\ &= -\bar{\tilde{C}} P_R C^T \bar{d}^T \tilde{u} = -\bar{\tilde{C}} P_R C^T \bar{d}^T \tilde{u} \\ &= \bar{\tilde{C}} P_R d^c \tilde{u} \end{aligned} \quad (\text{A.7})$$

When contracting this operator with the $\tilde{N}\tilde{C}W^+$ vertex we get the opposite spin structure,

$$\begin{aligned} \mathcal{M}_{\tilde{u}} &= g_2^2 V_{11} \bar{u}_{\tilde{N}}(p_4) \gamma^\mu (\mathcal{O}_{11}^L P_L + \mathcal{O}_{11}^R P_R) \frac{\not{q} + M_{\tilde{C}}}{q^2 - M_{\tilde{C}}^2} P_R v_d(p_2) \epsilon_\mu(p_3) \\ &= V_{11} \bar{u}_{\tilde{N}}(p_4) \gamma^\mu \frac{b\not{q} + aM_{\tilde{C}}}{q^2 - M_{\tilde{C}}^2} v_u(p_2) \epsilon_\mu(p_3) \end{aligned} \quad (\text{A.8})$$

Experimentally, we cannot distinguish between up quarks and down quarks. We must therefore average over the two contributions,

$$\sum_{\tilde{u}, \tilde{d}} |\mathcal{M}|^2 \propto (b^2 - a^2)(f_d(U_{11}^*)^2 - f_u(V_{11})^2) t_{qW} + \text{Const.} \quad (\text{A.9})$$

f_d and f_u is the fraction of events with a down-squark or up-squark, respectively.

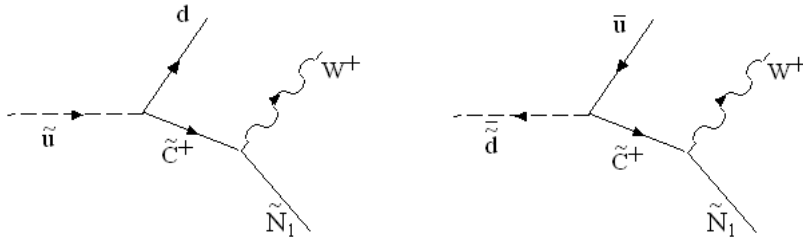


Figure 21: Two different process contributing to squark decay into \tilde{C}^+ and a quark. The chargino consequently decays into W^\pm and LSP.

B. HERWIG implementation

In this appendix we review the implementation of matrix elements into HERWIG. This section is relevant to any Monte-Carlo program using the S and F functions of Eijk and Kleiss [35] to calculate helicity amplitudes. The usage of these functions results in very efficient computations. The price the user has to pay is the complexity of the expressions. These functions are then used in the spin correlations algorithm devised by Knowles and Collins [25, 28]. We hope to provide a brief but fairly self-consistent presentation below.

HERWIG is an event generator consisting of roughly 5 phases (for a complete description of the program consult [24]):

1. Hard process, where the particles in the main $2 \rightarrow 2, 3$ event are generated, e.g. $q q \rightarrow g g$ or $e^+ e^- \rightarrow q \bar{q}$.
2. The parton shower phase involving the QCD evolution from the collision energy to the infrared cutoff.
3. Decay of heavy unstable particles before hadronization, such as top quark and SUSY partners.
4. Hadronization stage
5. Decay of unstable hadrons.

We are mainly concerned with the third step. In order to decay any unstable particle (e.g. gluino, squark etc.), one must provide HERWIG with its different decay channels and the corresponding matrix elements. To keep track of spin correlations the matrix element must include the external polarizations. For example, let's consider the decay of a heavy fermion into a fermion and a scalar (top decay into bottom and higgs). The matrix element is given by,

$$i\mathcal{M} = ig\bar{u}(q, \lambda_2)u(p, \lambda_1) \tag{B.1}$$

In order to compute this spinor product, HERWIG requires the user to express it in terms of the S and F functions of Eijk and Kleiss [35] defined below. This facilitates the algebra, but obscures the expression. Let's briefly recall the construction.

One begins by expressing any polarization in terms of massless spinors (for a pedagogical review, see [36]). Two basic 4-momenta, k_0, k_1 are chosen such that,

$$k_0 \cdot k_0 = 0, k_0 \cdot k_1 = 0, k_1 \cdot k_1 = -1 \tag{B.2}$$

The basic left and right helicities are then defined via,

$$u_L(k_0)\bar{u}_L(k_0) = P_L \not{k}_0, \quad u_R(k_0) = \not{k}_1 u_L(k_0) \tag{B.3}$$

The helicity spinor for any other momenta (not collinear with k_0) is then given by,

$$u_\lambda(k) = \not{k} u_{-\lambda}(k_0) / \sqrt{2k_0 \cdot k} \tag{B.4}$$

A massive spinor is nothing but the linear combination of two massless spinors of opposite helicities. It can be written as,

$$\begin{aligned} u(p, \lambda) &= \frac{(\not{p} + m) u_{-\lambda}(k_2)}{\sqrt{2p \cdot k_2}} \\ &= \frac{1}{\sqrt{2p \cdot k_2}} (S_\lambda(k_1, k_2) u_\lambda(k_1) + m u_{-\lambda}(k_2)) \end{aligned} \tag{B.5}$$

where $p = k_1 + k_2$ is decomposed into two massless 4-vectors and the S function is defined as,

$$S_\lambda(k_1, k_2) = \bar{u}_\lambda(k_1) u_{-\lambda}(k_2) = (S_{-\lambda}(k_2, k_1))^* = -S_\lambda(k_2, k_1) \tag{B.6}$$

Notice that, $|S_\lambda(k_1, k_2)|^2 = m^2$.

All expressions can therefore be reduced into products of massless spinors, with the possibility of having a γ^μ matrix sandwiched in between. It proves useful to define the F function as well,

$$F(k_1, \lambda_1, p, k_2, \lambda_2, M) = \bar{u}_{\lambda_1}(k_2) (\not{p} + M) u_{\lambda_2}(k_1) \tag{B.7}$$

for some p which is not light-like. Matrix elements for many typical processes were already implemented in HERWIG by P. Richardson. As an example, the above matrix element (B.1) can be written as,

$$\begin{aligned} \mathcal{M} &= g \bar{u}(q, \lambda_2) u(p, \lambda_1) \\ &= g \frac{1}{\sqrt{2p \cdot p_2}} \frac{1}{\sqrt{2q \cdot q_2}} (S_{\lambda_2}^*(q_1, q_2) \bar{u}_{\lambda_2}(q_1) + m_2 \bar{u}_{-\lambda_2}(q_2)) (\not{p} + m_1) u_{-\lambda_1}(p_2) \\ &= \frac{1}{\sqrt{2p \cdot p_2}} \frac{1}{\sqrt{2q \cdot q_2}} \\ &\quad \times g (S_{-\lambda_2}(q_2, q_1) F(q_1, \lambda_2, p, p_2, -\lambda_1, m_1) + m_2 F(q_2, -\lambda_2, p, p_2, -\lambda_1, m_1)) \end{aligned}$$

For a massless spin-1 particle the external polarization $\epsilon^\mu(k, \lambda)$ can be expressed as,

$$\epsilon^\mu(k, \lambda) = \bar{u}_\lambda(k) \gamma^\mu u_\lambda(k_1) / \sqrt{4k \cdot k_1} \tag{B.8}$$

where k_1 is any light-like momentum not collinear with k .

The extra polarization of a massive spin-1 particle adds an extra complication to the calculation. Since the only massive gauge bosons in the MSSM are the W^\pm and Z , it is easier to simply insert the entire matrix element (e.g. $t \rightarrow b + e^+ + \nu_e$ rather than $t \rightarrow b + W^+$ and $W^+ \rightarrow e^+ + \nu_e$). In Same-Spin theories, there are many massive gauge bosons around and it proves useful to develop the needed formalism and implement it in HERWIG.

Looking at the massless polarization (B.8) it is easy to guess the form of a massive one in terms of spinors,

$$\epsilon^\mu(p, \lambda_1, \lambda_2) = \frac{1}{(2\sqrt{2}m)} \bar{u}(p, \lambda_1) \gamma^\mu v(p, \lambda_2) \quad (\text{B.9})$$

where, $p^2 = m^2$ and $\lambda_{1,2}$ are the usual spinor polarizations. This might seem wrong at first, as it seems to imply 4 polarizations rather than the required 3, but as we will see in a moment, $(+, +)$ and $(-, -)$ both correspond to the scalar polarization. First, let's verify that this indeed reproduces the correct polarization sum,

$$\sum_{\lambda_1, \lambda_2} \epsilon_\mu(p, \lambda_1, \lambda_2) \epsilon_\nu^*(p, \lambda_1, \lambda_2) / (8m^2) = \sum_{\lambda_1, \lambda_2} \text{Tr}(u(p, \lambda_1) \bar{u}(p, \lambda_1) \gamma_\mu v(p, \lambda_2) \bar{v}(p, \lambda_2) \gamma_\nu) / (8m^2)$$

$$= \text{Tr}((\not{p} + m) \gamma_\mu (\not{p} - m) \gamma_\nu) / (8m^2) \quad (\text{B.10})$$

$$= \left(-g_{\mu\nu} + \frac{p_\mu p_\nu}{m^2} \right) \quad (\text{B.11})$$

It is straight forward to show that (B.9) corresponds to the different polarizations directly. First note that,

$$\begin{aligned} \epsilon_\mu(p, \lambda_1, \lambda_2) &= \frac{1}{2\sqrt{2}m} \frac{1}{2p \cdot p_1} \\ &\times (S_{\lambda_1}^*(p_1, p_2) \bar{u}_{\lambda_1}(p_1) + m \bar{u}_{-\lambda_1}(p_2)) \gamma_\mu (S_{\lambda_2}(p_1, p_2) u_{\lambda_2}(p_1) - m u_{-\lambda_2}(p_2)) \\ &= \begin{cases} \bar{u}_\lambda(p_1) \gamma_\mu u_\lambda(p_1) - \bar{u}_\lambda(p_2) \gamma_\mu u_\lambda(p_2) / 2\sqrt{2}m & \lambda_1 \equiv \lambda = \lambda_2 \\ \frac{(S_{-\lambda} - S_\lambda^*)}{m} \bar{u}_\lambda(p_2) \gamma_\mu u_\lambda(p_1) / 2\sqrt{2}m & \lambda_1 \equiv \lambda \neq \lambda_2 \end{cases} \end{aligned}$$

In the rest frame of the particle we can take $\vec{p}_1 = \hat{z}|p|/2$ and $\vec{p}_2 = -\hat{z}|p|/2$, so that $p = p_1 + p_2 = (m, \vec{0})$ and the massless spinors are given by,

$$u_-(p_1) = \sqrt{2m} \begin{pmatrix} 0 \\ 1 \\ 0 \\ 0 \end{pmatrix} \quad u_+(p_1) = \sqrt{2m} \begin{pmatrix} 0 \\ 0 \\ 1 \\ 0 \end{pmatrix} \quad (\text{B.12})$$

With a few lines of arithmetic one can verify that,

$$\epsilon_\mu(p, -, -) = ((1, 0, 0, m) - (1, 0, 0, -m)) / (2\sqrt{2}m) = (0, 0, 0, 1/\sqrt{2})$$

$$\epsilon_\mu(p, +, +) = ((1, 0, 0, m) - (1, 0, 0, -m)) / (2\sqrt{2}m) = (0, 0, 0, 1/\sqrt{2})$$

$$\epsilon_\mu(p, -, +) = 2(0, m, im, 0) / (2\sqrt{2}m) = (0, 1/\sqrt{2}, i/\sqrt{2}, 0)$$

$$\epsilon_\mu(p, +, -) = 2(0, m, -im, 0) / (2\sqrt{2}m) = (0, 1/\sqrt{2}, -i/\sqrt{2}, 0)$$

and so we conclude that $\epsilon^\mu(-, +) = \epsilon_L^\mu$, $\epsilon^\mu(+, -) = \epsilon_R^\mu$ and $\epsilon^\mu(-, -) = \epsilon^\mu(+, +) = \epsilon_0^\mu/\sqrt{2}$. It is now straight forward, albeit tedious, to express any matrix element involving an external massive gauge boson in terms of S and F functions and implement it into HERWIG.

We begin with the matrix element for a gauge boson decay into a fermion - anti-fermion pair,

$$i\mathcal{M} = iA_\lambda \bar{u}(k, \lambda_2) \gamma^\mu P_\lambda v(q, \lambda_4) \epsilon_\mu(p, \lambda_1, \lambda_2) \quad (\text{B.13})$$

The corresponding expressions are,

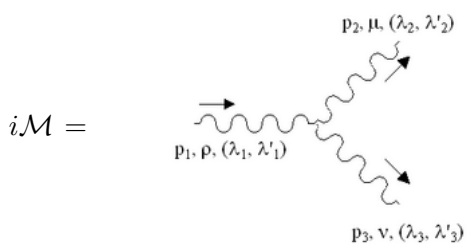
$$\begin{aligned} \mathcal{M}((\lambda_1, \lambda_1), \lambda_3, \lambda_4) &= \frac{\sqrt{2}}{\sqrt{4p \cdot p_2 2k \cdot k_2 2q \cdot q_2}} \\ &\times (A_{-\lambda_1}(F(k_2, -\lambda_3, k, p_1, \lambda_1, m_2)F(p_1, \lambda_1, q, q_2, -\lambda_4, -m_3) + (p_1 \rightarrow p_2)) \\ &+ (\lambda_1 \rightarrow -\lambda_1)) \\ \mathcal{M}((\lambda_1, -\lambda_1), \lambda_3, \lambda_4) &= \frac{1}{\sqrt{4p \cdot p_2 2k \cdot k_2 2q \cdot q_2}} \\ &\times \left(\frac{S_{-\lambda_1}(p_1, p_2) - S_{\lambda_1}^*(p_1, p_2)}{m_1} \right) \\ &\times (A_{-\lambda_1}F(k_2, -\lambda_3, k, p_2, \lambda_1, m_2)F(p_1, \lambda_1, q, q_2, -\lambda_4, -m_3) \\ &+ (p_1 \leftrightarrow p_2, \lambda_1 \rightarrow -\lambda_1)) \end{aligned}$$

The factor of $\sqrt{2}$ above is to guarantee proper normalization of the longitudinal mode. With a little bit of care it is easy to obtain the other two diagrams $f(\bar{f}) \rightarrow f(\bar{f}) + g.b..$ To turn a fermion into an anti-fermion or vice-versa simply send $m \rightarrow -m$. The incoming gauge-boson polarization becomes an outgoing one by conjugation,

$$\epsilon_\mu \rightarrow \epsilon_\mu^* = \bar{v}(p, \lambda_2) \gamma_\mu u(p, \lambda_1) = \lambda_1 \lambda_2 \bar{u}(p, -\lambda_1) \gamma_\mu v(p, -\lambda_2) \quad (\text{B.14})$$

So we simply have to send $\lambda_1 \rightarrow -\lambda_1$ in the expressions above, and an overall minus sign in front of the $\mathcal{M}((\lambda_1, -\lambda_1), \lambda_3, \lambda_4)$ amplitude due to the $\lambda_1 \lambda_2$ factor.

The last diagram we consider is the non-Abelian vertex including 3 external massive spin-1 polarizations.



$$= ig (g^{\mu\nu} (p_3 - p_2)^\rho + g^{\nu\rho} (-p_1 - p_3)^\mu + g^{\rho\mu} (p_2 + p_1)^\nu) \quad (\text{B.15})$$

$$\times \epsilon_\rho(p_1, \lambda_1, \lambda'_1) \epsilon_\mu^*(p_2, \lambda_2, \lambda'_2) \epsilon_\nu^*(p_3, \lambda_3, \lambda'_3) \quad (\text{B.16})$$

We give the corresponding expression for the first term only. The other terms can be obtained by trivial permutations and using (B.14) for the outgoing polarizations.

$$\begin{aligned} i\mathcal{M} &\supset \epsilon_\mu^*(p_2, \lambda_2, \lambda'_2) \epsilon_\nu^*(p_3, \lambda_3, \lambda'_3) g^{\mu\nu} (p_3 - p_2)^\rho \epsilon_\rho(p_1, \lambda_1, \lambda'_1) \\ &= \frac{1}{16\sqrt{2}m_1 m_2 m_3} A(\lambda_2, \lambda'_2, \lambda_3, \lambda'_3) B(\lambda_1, \lambda'_1) \end{aligned} \quad (\text{B.17})$$

where,

$$A(\lambda_2, \lambda'_2, \lambda_3, \lambda'_3) = \begin{cases} \lambda_2 = \lambda'_2 & \frac{1}{m_3^2} (F(q'_3, \lambda_3, p_3, q_2, \lambda_2, m_3)F(q_2, \lambda_2, p_3, q'_3, \lambda'_3, -m_3) \\ & - F(q'_3, \lambda_3, p_3, q'_2, \lambda_2, m_3)F(q'_2, \lambda_2, p_3, q'_3, \lambda'_3, -m_3) \\ & + \lambda_3 \rightarrow -\lambda_3) \\ \lambda_2 = -\lambda'_2 & \frac{1}{m_3^2} \left(\frac{S(q_2, q'_2, -\lambda_2) - S^*(q_2, q'_2, \lambda_2)}{m_2} \right) \times \\ & (F(q'_3, \lambda_3, p_3, q'_2, \lambda_2, m_3)F(q_2, \lambda_2, p_3, q'_3, \lambda'_3, -m_3) \\ & + (\lambda_3 \rightarrow -\lambda_3, q'_2 \leftrightarrow q_2)) \end{cases}$$

and,

$$B(\lambda_1, \lambda'_1) = \begin{cases} \lambda_1 = \lambda'_1 & (F(q_1, \lambda_1, p_3 - p_2, q_1, \lambda_1, 0) - F(q'_1, -\lambda_1, p_3 - p_2, q'_1, -\lambda_1, 0)) \\ \lambda_1 = -\lambda'_1 & \left(\frac{S(q_1, q'_1, -\lambda_1) - S^*(q_1, q'_1, \lambda_1)}{m_1} F(q_1, \lambda_1, p_3 - p_2, q'_1, \lambda_1, 0) \right) \end{cases}$$

Here, the momenta is written in terms of two massless momenta $p_i = q_i + q'_i$, with $q_i^2 = (q'_i)^2 = 0$ and $p_i^2 = m_i^2$.

References

- [1] H. Baer, C.-h. Chen, F. Paige and X. Tata, *Signals for minimal supergravity at the cern Large Hadron Collider: multi-jet plus missing energy channel*, *Phys. Rev. D* **52** (1995) 2746 [[hep-ph/9503271](#)].
- [2] H. Baer, C.-h. Chen, F. Paige and X. Tata, *Signals for minimal supergravity at the Cern large hadron collider II: multilepton channels*, *Phys. Rev. D* **53** (1996) 6241 [[hep-ph/9512383](#)].
- [3] I. Hinchliffe, F.E. Paige, M.D. Shapiro, J. Soderqvist and W. Yao, *Precision SUSY measurements at LHC*, *Phys. Rev. D* **55** (1997) 5520 [[hep-ph/9610544](#)].
- [4] I. Hinchliffe et al., *Precision SUSY measurements at LHC: Point 3*, LBNL-40954.
- [5] *Atlas detector and physics performance. technical design report. vol. 1 and 2*, CERN-LHCC-99-15.
- [6] C.G. Lester and D.J. Summers, *Measuring masses of semi-invisibly decaying particles pair produced at hadron colliders*, *Phys. Lett. B* **463** (1999) 99 [[hep-ph/9906349](#)].
- [7] C.G. Lester, M.A. Parker and M.J. White, *Determining SUSY model parameters and masses at the LHC using cross-sections, kinematic edges and other observables*, *JHEP* **01** (2006) 080 [[hep-ph/0508143](#)].
- [8] D.J. Miller, P. Osland and A.R. Raklev, *Invariant mass distributions in cascade decays*, *JHEP* **03** (2006) 034 [[hep-ph/0510356](#)].
- [9] N. Arkani-Hamed, G.L. Kane, J. Thaler and L.-T. Wang, *Supersymmetry and the LHC inverse problem*, *JHEP* **08** (2006) 070 [[hep-ph/0512190](#)].
- [10] N. Arkani-Hamed, A.G. Cohen and H. Georgi, *(de)constructing dimensions*, *Phys. Rev. Lett.* **86** (2001) 4757 [[hep-th/0104005](#)].

- [11] T. Appelquist, H.-C. Cheng and B.A. Dobrescu, *Bounds on universal extra dimensions*, *Phys. Rev. D* **64** (2001) 035002 [[hep-ph/0012100](#)].
- [12] H.-C. Cheng and I. Low, *TeV symmetry and the little hierarchy problem*, *JHEP* **09** (2003) 051 [[hep-ph/0308199](#)].
- [13] H.-C. Cheng and I. Low, *Little hierarchy, little higgses and a little symmetry*, *JHEP* **08** (2004) 061 [[hep-ph/0405243](#)].
- [14] I. Low, *T parity and the littlest Higgs*, *JHEP* **10** (2004) 067 [[hep-ph/0409025](#)].
- [15] H.-C. Cheng, I. Low and L.-T. Wang, *Top partners in little Higgs theories with t-parity*, *Phys. Rev. D* **74** (2006) 055001 [[hep-ph/0510225](#)].
- [16] A. Datta, G.L. Kane and M. Toharia, *Is it SUSY?*, [hep-ph/0510204](#).
- [17] P. Meade and M. Reece, *Top partners at the LHC: spin and mass measurement*, *Phys. Rev. D* **74** (2006) 015010 [[hep-ph/0601124](#)].
- [18] A.J. Barr, *Using lepton charge asymmetry to investigate the spin of supersymmetric particles at the LHC*, *Phys. Lett. B* **596** (2004) 205 [[hep-ph/0405052](#)].
- [19] A. Datta, K. Kong and K.T. Matchev, *Discrimination of supersymmetry and universal extra dimensions at hadron colliders*, *Phys. Rev. D* **72** (2005) 096006 [[hep-ph/0509246](#)].
- [20] J.M. Smillie and B.R. Webber, *Distinguishing spins in supersymmetric and universal extra dimension models at the Large Hadron Collider*, *JHEP* **10** (2005) 069 [[hep-ph/0507170](#)].
- [21] A. Alves, O. Eboli and T. Plehn, *It's a gluino*, *Phys. Rev. D* **74** (2006) 095010 [[hep-ph/0605067](#)].
- [22] H.-C. Cheng, K.T. Matchev and M. Schmaltz, *Bosonic supersymmetry? getting fooled at the LHC*, *Phys. Rev. D* **66** (2002) 056006 [[hep-ph/0205314](#)].
- [23] B.C. Allanach et al., *The snowmass points and slopes: benchmarks for SUSY searches*, [hep-ph/0202233](#).
- [24] G. Corcella et al., *Herwig 6.5 release note*, [hep-ph/0210213](#).
- [25] J.C. Collins, *Spin correlations in Monte Carlo event generators*, *Nucl. Phys. B* **304** (1988) 794.
- [26] I.G. Knowles, *Angular correlations in QCD*, *Nucl. Phys. B* **304** (1988) 767.
- [27] I.G. Knowles, *A linear algorithm for calculating spin correlations in hadronic collisions*, *Comput. Phys. Commun.* **58** (1990) 271.
- [28] I.G. Knowles, *Spin correlations in parton-parton scattering*, *Nucl. Phys. B* **310** (1988) 571.
- [29] P. Richardson, *Spin correlations in Monte Carlo simulations*, *JHEP* **11** (2001) 029 [[hep-ph/0110108](#)].
- [30] A.J. Barr, *Measuring slepton spin at the LHC*, *JHEP* **02** (2006) 042 [[hep-ph/0511115](#)].
- [31] D.J.H. Chung et al., *The soft supersymmetry-breaking Lagrangian: theory and applications*, *Phys. Rept.* **407** (2005) 1 [[hep-ph/0312378](#)].
- [32] V.D. Barger and R.J.N. Phillips, *Collider physics*, Redwood City, U.S.A., Addison-Wesley (1987).

- [33] C. Macesanu, C.D. McMullen and S. Nandi, *Collider implications of models with extra dimensions*, hep-ph/0211419.
- [34] T. Han, private communication.
- [35] B. van Eijk and R. Kleiss, *On the calculation of the exact $gg \rightarrow ZB\bar{B}$ cross-section including Z decay and B quark mass effects*, in *Aachen, Proceedings, Large Hadron Collider*, **2** (1990) 183, CERN Geneva - CERN-90-10-B (90/12,rec.Jul.91) 183.
- [36] R. Kleiss and W.J. Stirling, *Spinor techniques for calculating $p\bar{p} \rightarrow w^\pm/Z^0 + \text{jets}$* , *Nucl. Phys.* **B 262** (1985) 235.